Jill Key

Chapter 6
Kiribati

6.1 Climate Summary

6.1.1 Current Climate

- Warming trends are evident in both annual and half-year mean air temperatures at Tarawa from 1950.
- At Kiritmati, in eastern Kiribati, there has been an increase in November–April rainfall since 1946. This implies either a shift in the mean location of the Inter-Tropical Convergence Zone (ITCZ) towards Kiritimati and/or a change in the intensity of rainfall associated with the ITCZ. The remaining annual and seasonal rainfall trends for Kiritimati and Tarawa and the extreme rainfall trends for Tarawa show little change.
- At Kiritmati, in eastern Kiribati, there has been an increase in November–April rainfall since 1946. This implies either a shift in the mean location of the ITCZ towards Kiritimati and/or a change in the intensity of rainfall associated with the ITCZ. The remaining annual and seasonal rainfall trends for Kiritimati and Tarawa and the extreme rainfall trends for Tarawa show little change.
- Wind-waves in Kiribati are strongly influenced by both north-easterly and south-easterly trade winds seasonally, and the location of the South Pacific Convergence Zone (SPCZ), with some effect of the El Niño–Southern Oscillation (ENSO) interannually. There is little variation in wave climate across the country. Available data are not suitable for assessing long-term trends (see Section 1.3).

6.1.2 Climate Projections

For the period to 2100, the latest global climate model (GCM) projections and climate science findings indicate:

- El Niño and La Niña events will continue to occur in the future (*very high confidence*), but there is little consensus on whether these events will change in intensity or frequency;
- Annual mean temperatures and extremely high daily temperatures will continue to rise (*very high confidence*);
- Average rainfall is projected to increase (*high confidence*), along with more extreme rain events *(high confidence*);
- Droughts are projected to decline in frequency (*medium confidence*);
- Ocean acidification is expected to continue *(very high confidence);*
- The risk of coral bleaching will increase in the future (*very high confidence);*
- Sea level will continue to rise *(very high confidence); and*
- Wave height is projected to decrease in December–March (*low confidence)*, waves may be more directed from the south in October *(low confidence)*.

6.2 Data Availability

There are currently five operational meteorological stations in Kiribati. Tarawa, the primary station, is located on the southern side of Tarawa Atoll at Betio in the Gilbert Islands. Kiritimati, the primary station in the Line Islands, is situated on the north-west side of the Kiritimati Atoll. All five operational stations, including Banaba and Tabuaeran, have rainfall records which begin between 1909 and 1945. Banaba has the earliest temperature record which began in 1909 but closed in 1993. Tarawa, Beru and Kanton (also known as Canton) have temperature records from 1947. Some temperature data are available for Kiritimati but these records are insufficient for analysis.

Tarawa rainfall from 1947, air temperature from 1950, and Kiritimati monthly rainfall from 1946, have been used in this report. These records are homogeneous. Additional information on historical climate trends in the Kiribati region can be found in the Pacific Climate Change Data Portal www.bom.gov.au/climate/pccsp/.

Wind-wave data from buoys are particularly sparse in the Pacific region, with very short records. Model and reanalysis data are therefore required to detail the wind-wave climate of the region. Reanalysis surface wind data have been used to drive a wave model over the period 1979–2009 to generate a hindcast of the historical wind-wave climate.

6.3 Seasonal Cycles

Information on temperature and rainfall seasonal cycles can be found in Australian Bureau of Meteorology and CSIRO (2011).

6.3.1 Wind-driven Waves

Surface wind-wave driven processes can impact on many aspects of Pacific Island coastal environments, including: coastal flooding during storm wave events; coastal erosion, both during episodic storm events and due to long-term changes in integrated wave climate; characterisation of reef morphology and marine habitat/species distribution; flushing and circulation of lagoons; and potential shipping and renewable wave energy solutions. The surface offshore wind-wave climate can be described by characteristic wave heights, lengths or periods, and directions.

The wind-wave climate of Kiribati shows only a little spatial variability across the region despite its large extent.

Waves in the Gilbert Islands are strongly characterised by trade winds, with waves coming from the north-east to east in December–March and the east and south-east during June–September.

Phoenix Islands similarly experience waves characterised by trade winds, but with northerly swell in December–March from north Pacific-generated storm waves, and south-east swell in June–September.

Waves in the Line Islands are similar, being from the north-east to east in December–March and slightly south of east in June–September due to trade winds, with swell from the north-west to north-east in December–March resulting from north Pacific storms, and south to south-easterly swell in June–September.

In the west, e.g. off the south-east coast of Tarawa, waves are characterised by variability of the trade winds, both north and south, with some swell from extra-tropical storms. During the northern trade wind season, December–March, waves at Tarawa have a slightly larger height and longer period than in other months (mean height around 1.8 m and period around 8.7 s) (Figure 6.1 and Table 6.1). In the southern trade wind season, June–September, waves have a slightly shorter period (mean around 8.3 s) and lower height (mean around 1.4 m) than December–March (Table 6.1). These waves consist of locally generated trade wind waves from the east and north-east in December–March and from the east and south-east during June–September, as well as trade wind induced swell, and some swell propagating from extra-tropical storms in the North Pacific and Southern Ocean. Waves larger than 2.5 m (99th percentile) occur usually from the east-northeast, in any month, with some large west and north-westerly waves due to extra-tropical storms in the north Pacific in northern winter months. The height of a 1-in-50 year wave event at the south-east coast of Tarawa is calculated to be 3.6 m.

In the east, e.g. off the north-west coast of Kiritimati, waves are characterised by trade winds seasonally. Waves come from the north-east during the northern trade wind season, December–March, with some small south-easterly waves, and both north-east and north-west swell from trade winds and extra-tropical storms. Most south-east trade wind waves in June–September are blocked by the island, with some small locally generated trade wind waves, and southerly swell from Southern Ocean storms observed (Figure 6.2). Wave heights also vary seasonally, reaching a maximum height in December–March (mean wave height 1.8 m), with smaller average waves in June–September (seasonal mean wave height 1.4 m) (Table 6.1).

There is no significant variation in wave period. Waves larger than 2.6 m (99th percentile) at Kiritimati occur predominantly during December–March and have periods of between 9 and 17s, usually directed from the north due to North Pacific storms, with some large waves directed from the south observed during other months (February, April-June) and from the west in February and October. The height of a 1-in-50 year wave event is calculated to be 3.9 m.

No suitable dataset is available to assess long-term historical trends in the Kiribati wave climate. However, interannual variability may be assessed in the hindcast data. The wind-wave climate displays interannual variability at both Tarawa and Kiritimati, varying with the El Niño–Southern Oscillation (ENSO). During La Niña years, wave power at Tarawa is around 35% greater than during El Niño years in June–September but slightly less in December–March, with waves more strongly directed from the east, associated with increased trade wind speeds. To the north-west of Kiritimati, wave power is slightly greater during La Niña years in June–September than in El Niño years, but is ~20% less in December–March than in El Niño years. Due to increased trade winds, waves are directed more from the east in La Niña years. Location of the SPCZ over a region may suppress locally generated waves. When the Southern Annular Mode (SAM) index is negative, waves at Kiritimati are directed more from the west in December–March due to propagation of swell from increased mid-latitude storms in the Southern Ocean.

Table 6.1: Mean wave height, period and direction from which the waves are travelling around Kiribati in December–March and June–September. Observation (hindcast) and climate model simulation mean values are given for Kiribati with the 5–95th percentile range (in brackets). Historical model simulation values are given for comparison with projections (see Section 6.5.6 – Wind-driven waves, and Tables 6.8, 6.9 and 6.10). A compass relating number of degrees to cardinal points (direction) is shown.

		Hindcast Reference Data (1979 2009),Tarawa	Climate Model Simulations (1986–2005) – Gilbert Islands	Climate Model Simulations (1986–2005) – Phoenix Islands	Hindcast Reference Data (1979–2009), Kiritimati	Climate Model Simulations (1986–2005) – Line Islands
Wave Height (metres)	December–March	1.8 (1.3–2.4)	1.9 (1.6–2.2)	2.0 (1.7–2.3)	1.8 (1.3–2.4)	2.0 (1.6–2.4)
	June–September	1.4 (1.0–1.9)	1.3 (1.2–1.5)	1.6 (1.4–1.8)	1.4 (1.0–1.9)	1.7 (1.5–2.0)
Wave Period (seconds)	December–March	8.7 (7.4–10.3)	8.8 (7.8–10.2)	9.7 (8.4–11.7)	10.6 (8.5–13.5)	9.8 (8.5–11.8)
	June–September	8.3 (7.0–9.8)	7.8 (7.1–8.7)	8.3 (7.3–9.3)	10.0 (7.5–13.1)	8.3 (7.4–9.4)
Wave direction (degrees clockwise from North)	December–March	60 (40–80)	50 (30–60)	30 (0–50)	10 (330–60)	30 (350–60)
	June–September	100 (80–120)	110 (90–120)	120 (110–130)	150 (60–210)	120 (110–140)

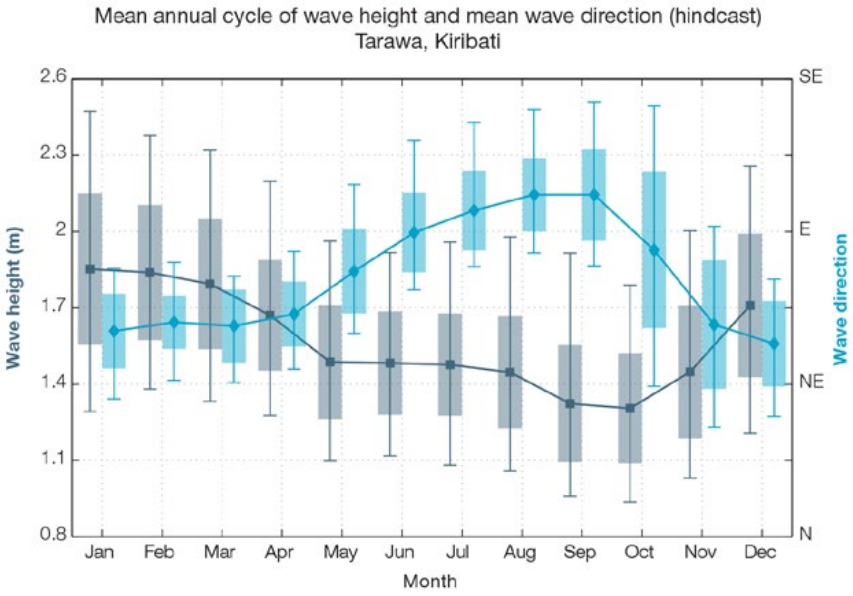

Figure 6.1: Mean annual cycle of wave height (grey) and mean wave direction (blue) at the south-east of Tarawa in hindcast data (1979–2009). To give an indication of interannual variability of the monthly means of the hindcast data, shaded boxes show 1 standard deviation around the monthly means, and error bars show the 5–95% range. The direction from which the waves are travelling is shown (not the direction towards which they are travelling).

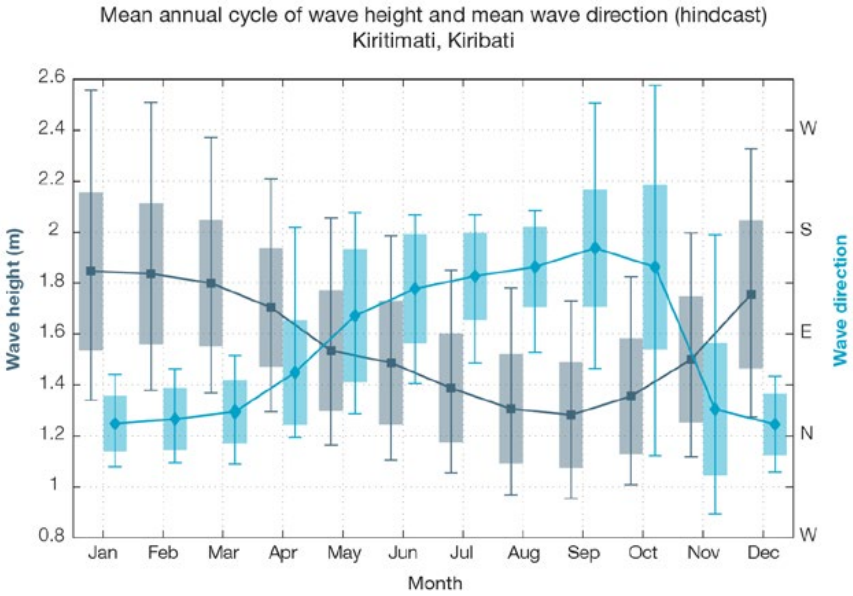

Figure 6.2: Mean annual cycle of wave height (grey) and mean wave direction (blue) off the north-west coast of Kiritimati in hindcast data (1979–2009). To give an indication of interannual variability of the monthly means of the hindcast data, shaded boxes show 1 standard deviation around the monthly means, and error bars show the 5–95% range. The direction from which the waves are travelling is shown (not the direction towards which they are travelling).

6.4 Observed Trends

6.4.1 Air Temperature

Annual and Half-year Mean Air Temperature

Warming trends of similar magnitude are evident in both annual and half-year mean air temperature at Tarawa for the period 1950–2011. Annual and November–April trends in maximum temperature are stronger than annual and November–April trends in minimum air temperatures (Figure 6.3 and Table 6.2).

Extreme Daily Air Temperature

Trends in extreme daily temperatures were all found to be positive but not statistically significant at the 5% level at Tarawa. Low temperature variability across the tropics means that trends in the absolute extreme temperature indices (i.e. Max Tmax, Max Tmin, Min Tmax, Min Tmin) are generally less than 0.1°C per decade, however, trends at Tarawa are particularly small. This is partly due to missing data in daily temperature record.

The strongest trends identified were in Max Tmin and Min Tmax. This shows that the warmest night-time temperature each year (Max Tmin) and the coolest day-time temperature each year (Min Tmax) have warmed. Mean annual maximum temperature shows a stronger warming compared to Max Tmax, with the warming in Min Tmax being of similar magnitude. This may be due to missing data but could also reflect that mean and cool extremes at Tarawa are warming more than the warm extremes.

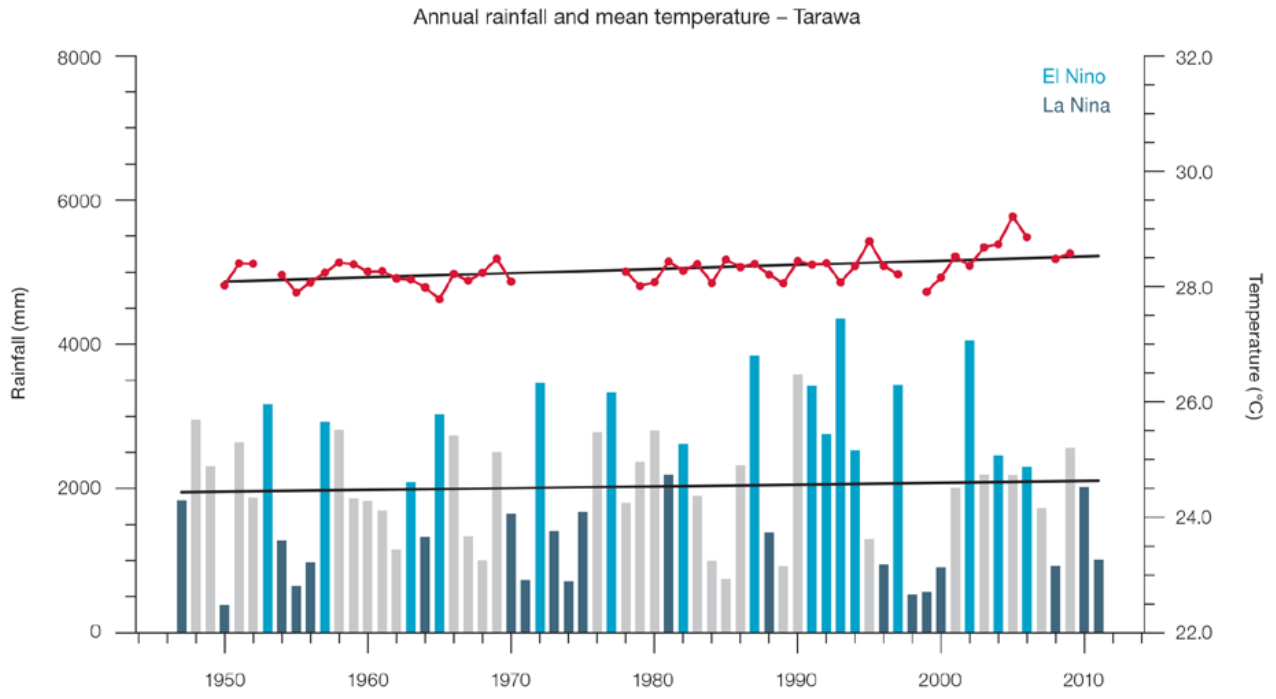

Figure 6.3: Observed time series of annual average values of mean air temperature (red dots and line) and total rainfall (bars) at Tarawa. Light blue, dark blue and grey bars denote El Niño, La Niña and neutral years respectively. Solid black trend lines indicate a least squares fit.

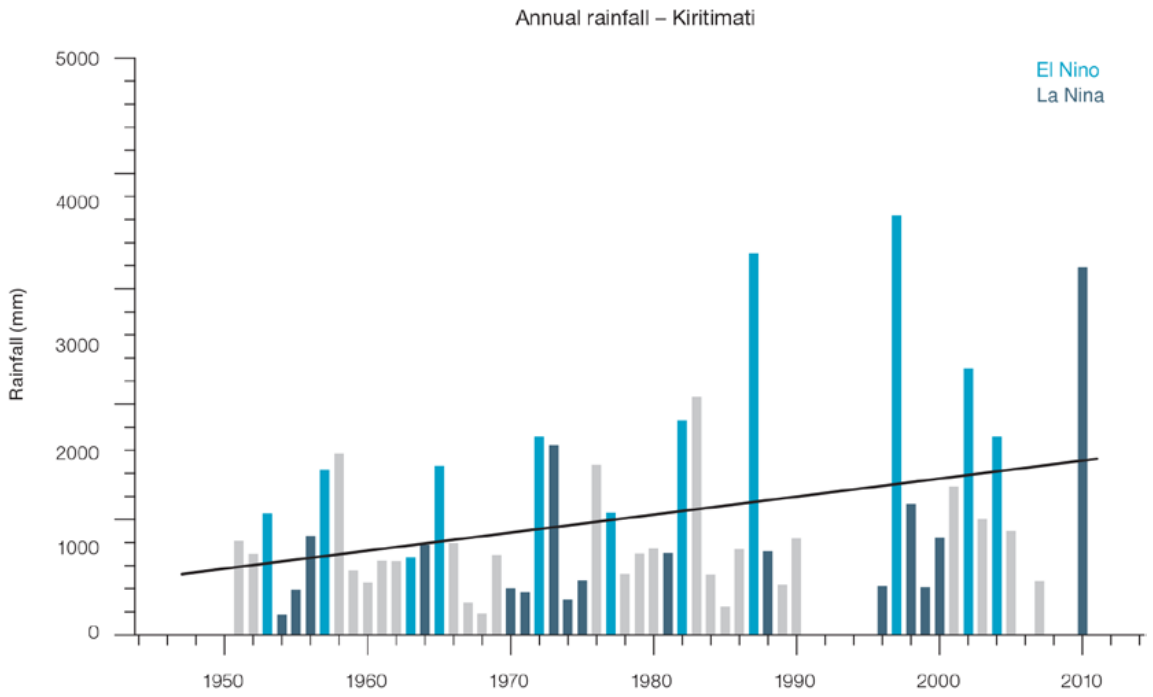

Figure 6.4: Observed time series of annual total rainfall (bars) at Kiritimati. Light blue, dark blue and grey bars denote El Niño, La Niña and neutral years respectively. Solid black trend lines indicate a least squares fit.

Table 6.2: Annual and half-year trends in air temperature (Tmax, Tmin, Tmean) and rainfall at Tarawa and Kiritimati. The 95% confidence intervals are shown in brackets. Values for trends significant at the 5% level are shown in **boldface**.

	Tarawa Tmax (°C/10yrs)	Tarawa Tmin (°C/10yrs)	Tarawa Tmean (°C/10yrs)	Tarawa Total Rain (mm/10yrs)	Kiritimati Total Rain (mm/10yrs)
		1950–2011		1947–2011	1946–2011
Annual	**+0.13** (+0.06, +0.21)	+0.04 (-0.07, +0.14)	**+0.08** (+0.01, +0.14)	-6.7 (-154.7, +156.9)	+84.2 (-4.4, +195.6)
Nov–Apr	**+0.16** (+0.06,+0.23)	+0.07 (-0.03, +0.17)	**+0.10** (+0.02, +0.18)	-17.4 (-133.3, +77.2)	**+58.0** (+2.2, +112.3)
May–Oct	+0.07 (-0.03, +0.17)	+0.05 (-0.03, +0.13)	**+0.07** (+0.01, +0.12)	+37.2 (-24.9, +97.0)	+10.3 (-15.2, +33.6)

Table 6.3: Annual trends in air temperature and rainfall extremes at Tarawa. The 95% confidence intervals are shown in brackets. None of the trends are significant at the 5% level.

	Tarawa
TEMPERATURE	**(1950–2011)**
Max Tmax (°C/decade)	0.05 (-0.10, +0.17)
Max Tmin (°C /decade)	0.14 (-0.02, +0.31)
Min Tmax (°C /decade)	0.12 (-0.01, 0.33)
Min Tmin (°C /decade)	0.08 (0, +0.12)
RAINFALL	**(1947–2011)**
Rain Days ≥ 1 mm (days/decade)	+3.54 (-3.05, +10.73)
Very Wet Day rainfall (mm/decade)	-20.78 (-74.19, +24.65)
Consecutive Dry Days (days/decade)	-1.01 (-3.03, +0.66)
Max 1-day rainfall (mm/decade)	-0.63 (-7.10, +5.24)

Minimum Tmin: Annual minimum value of minimum temperature
Maximum Tmin: Annual maximum value of maximum temperature
Minimum Tmax: Annual minimum value of maximum temperature
Maximum Tmax: Annual maximum value of maximum temperature
Rain Days ≥ 1 mm: Annual count of days where rainfall is greater or equal to 1 mm (0.039 inches)
Very Wet Day rainfall: Amount of rain in a year where daily rainfall is greater than the 95th percentile for the reference period 1971–2000
Consecutive Dry Days: Maximum number of consecutive days in a year with rainfall less than 1 mm (0.039 inches)
Max 1-day rainfall: Annual maximum 1-day rainfall

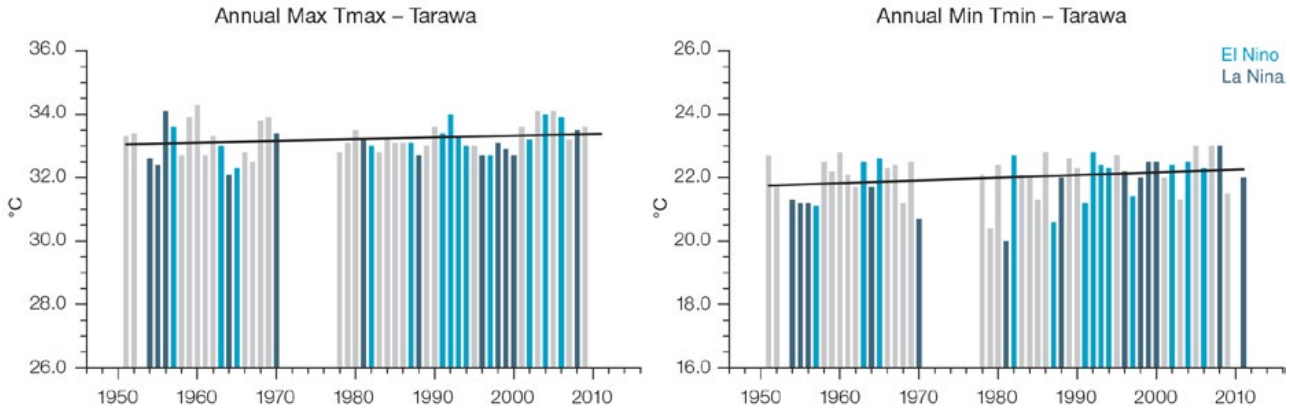

Figure 6.5: Observed time series of annual highest daily maximum temperature (Max Tmax - left) and Annual lowest daily minimum temperature (Min Tmin - right) at Tarawa. Solid black trend lines indicate a least squares fit.

6.4.2 Rainfall

Annual and Half-year Total Rainfall

Notable interannual variability associated with the ENSO is evident in the observed rainfall records for Tarawa since 1947 (Figure 6.3) and Kiritimati since 1946 (Figure 6.4). The positive trend in Kiritimati November—April rainfall (Table 6.2) is statistically significant at the 5% level. This implies either a shift in the mean location of the ITCZ or a change in the intensity of rainfall associated with the Inter-Tropical Convergence Zone. A daily rainfall record for the station is needed before changes in the intensity can be assessed. The ITCZ is closest to the equator in March–May, and furthest north during September–November, when it becomes broader, expanding both to the north and south.

The other total rainfall trends in Table 6.2, Figure 6.3 and Figure 6.4 are not statistically significant. In other words, excluding Kiritimati November–April rainfall, there has been little change in rainfall at Tarawa and Kiritimati.

Daily Rainfall

Daily rainfall trends for Tarawa are presented in Table 6.3. None of these trends are statistically significant. Figure 6.6 shows insignificant trends in the annual Consecutive Dry Days and Rain Days ≥ 1 mm.

6.4.3 Tropical Cyclones

As the Kiribati Islands are located within a few degrees of the equator, tropical cyclones rarely develop within or cross the Kiribati Exclusive Economic Zone (EEZ). The only recorded events are Cyclone Alice (1978/79) in the North Pacific (records from 1977–2011) and Cyclone Anne (1987/88) in the South Pacific (based on records from 1969/70 and 2010/11). Refer to Chapter 1, Section 1.4.2 (Tropical Cyclones) for an explanation of the difference in the number of tropical cyclones occurring in Kiribati in this report (Australian Bureau of Meteorology and CSIRO, 2014) compared to Australian Bureau of Meteorology and CSIRO (2011).

Additional information on historical tropical cyclones in the Kiribati region (Southern Hemisphere) can be found at www.bom.gov.au/cyclone/history/tracks/index.shtml

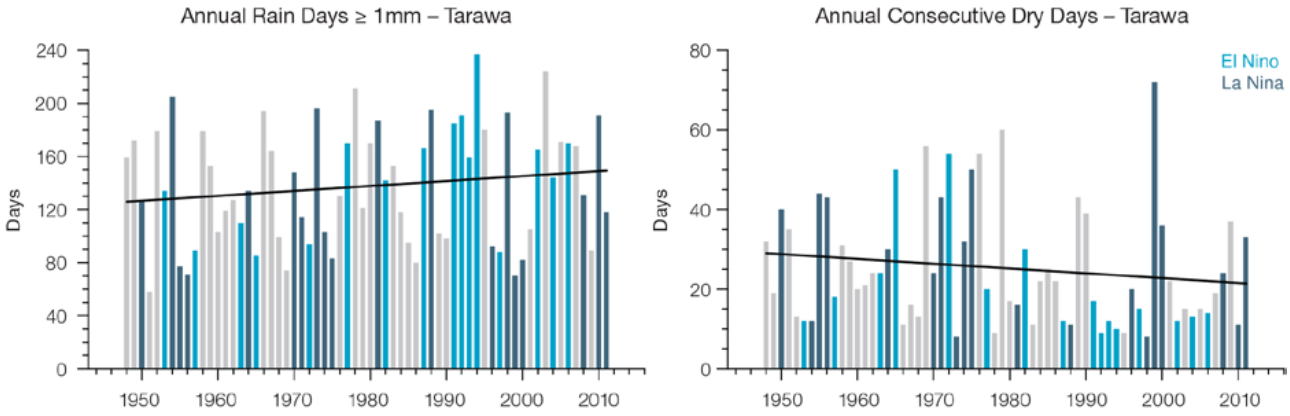

Figure 6.6: Observed time series of annual Rain Days ≥ 1 mm (left), and annual Consecutive Dry Days (right) at Tarawa. Solid black trend lines indicate a least squares fit.

6.5 Climate Projections

The performance of the available Coupled Model Intercomparison Project (Phase 5) (CMIP5) climate models over the Pacific has been rigorously assessed (Brown et al., 2013a, b; Grose et al., 2014; Widlansky et al., 2013). The simulation of the key processes and features for the Kiribati region is similar to the previous generation of CMIP3 models, with all the same strengths and many of the same weaknesses. The best-performing CMIP5 models used here have lower biases (differences between the simulated and observed climate data) than the best CMIP3 models, and there are fewer poorly-performing models. For Kiribati, the most important model bias is that islands are either along the equator where models have an ocean that is too cold with too little rainfall (the 'cold-tongue bias', also see Chapter 1), or within the SPCZ or ITCZ, where models overestimate rainfall. These issues mean that models have a bias in the temperature and rainfall in the present day and this affects the confidence in the model projections. Out of 27 models assessed, three models were rejected for use in these projections due to biases in the mean climate and in the simulation of the SPCZ. Climate projections have been derived from up to 24 new GCMs in the CMIP5 database (the exact number is different for each scenario, Appendix A), compared with up to 18 models in the CMIP3 database reported in Australian Bureau of Meteorology and CSIRO (2011).

It is important to realise that the models used give different projections under the same scenario. This means there is not a single projected future for Kiribati, but rather a range of possible futures for each emission scenario. This range is described below.

6.5.1 Temperature

Further warming is expected over Kiribati (Figure 6.7, Tables 6.5–6.7). Under all RCPs, the warming is up to 1.2°C by 2030, relative to 1995, but after 2030 there is a growing difference in warming between each RCP. For example, in the Gilbert Islands by 2090, a warming of 2.1–4.5°C is projected for RCP8.5 (very high emissions) while a warming of 0.6 to 1.5°C is projected for RCP2.6 (very low emissions), and there is a similar range in the Phoenix and Line Islands. This range is broader than that presented in Australian Bureau of Meteorology and CSIRO (2011) because a wider range of emissions scenarios is considered. While relatively warm and cool years and decades will still occur due to natural variability, there is projected to be more warm years and decades on average in a warmer climate.

There is *very high confidence* that temperatures will rise because:

- It is known from theory and observations that an increase in greenhouse gases will lead to a warming of the atmosphere; and
- Climate models agree that the long-term average temperature will rise.

There is *medium confidence* in the model average temperature change shown in Tables 6.5–6.7 because:

- The new models simulate the rate of temperature change of the recent past with reasonable accuracy;
- Sea-surface temperatures over the equator are too cold in most CMIP5 climate models in the current climate, including over some regions of the Line, Phoenix and Gilbert Groups, and this affects the projection into the future; and
- There is a bias in the simulation of the SPCZ and the ITCZ, affecting the uncertainty the projections of rainfall but also temperature. This is relevant to islands further from the equator.

6.5.2 Rainfall

The long-term average rainfall over much of Kiribati is projected by almost all models to increase. The increase is greater for the higher emissions scenarios, especially towards the end of the century (Figure 6.8, Tables 6.5-6.7). There is an increase projected for both the dry and wet season rainfall for all three island groups. The projected rainfall increase is greater in the Gilbert group and lower in the Line group. Mean rainfall decreased in the Line Islands and Phoenix Islands between 1979 and 2006 (Figure 6.8, middle and bottom panels), but the models do not project this will continue into the future. This indicates that the recent decrease may be caused by natural variability and not caused by global warming. It is also possible that the models do not simulate a key process driving the recent change. However, the recent change is not particularly large (<10%) and the observed record shown is not particularly long (28 years), so it is difficult to determine the significance of this difference, and its cause. There will still be wet and dry years and decades due to natural variability, but most models show that the long-term average is expected to be wetter. The effect of climate change on average rainfall may not be obvious in the short or medium term due to natural variability. These projections are similar to those in Australian Bureau of Meteorology and CSIRO (2011).

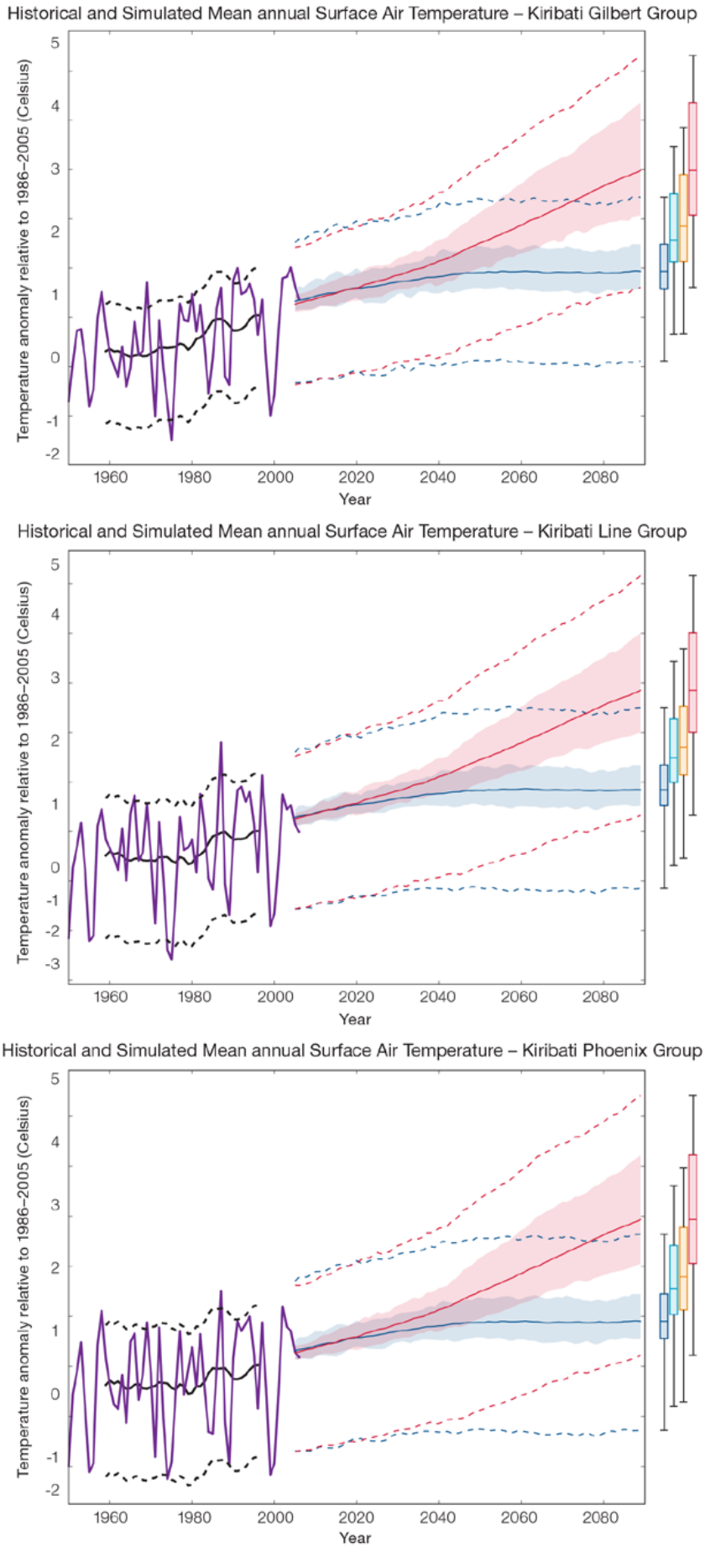

Figure 6.7: Historical and simulated surface air temperature time series for the region surrounding the Kiribati Gilbert Group (top), Line Group (middle) and Phoenix Group (bottom). The graph shows the anomaly (from the base period 1986–2005) in surface air temperature from observations (the GISS dataset, in purple), and for the CMIP5 models under the very high (RCP8.5, in red) and very low (RCP2.6, in blue) emissions scenarios. The solid red and blue lines show the smoothed (20-year running average) multi-model mean anomaly in surface air temperature, while shading represents the spread of model values (5–95th percentile). The dashed lines show the 5–95th percentile of the observed interannual variability for the observed period (in black) and added to the projections as a visual guide (in red and blue). This indicates that future surface air temperature could be above or below the projected long-term averages due to interannual variability. The ranges of projections for a 20-year period centred on 2090 are shown by the bars on the right for RCP8.5, 6.0, 4.5 and 2.6.

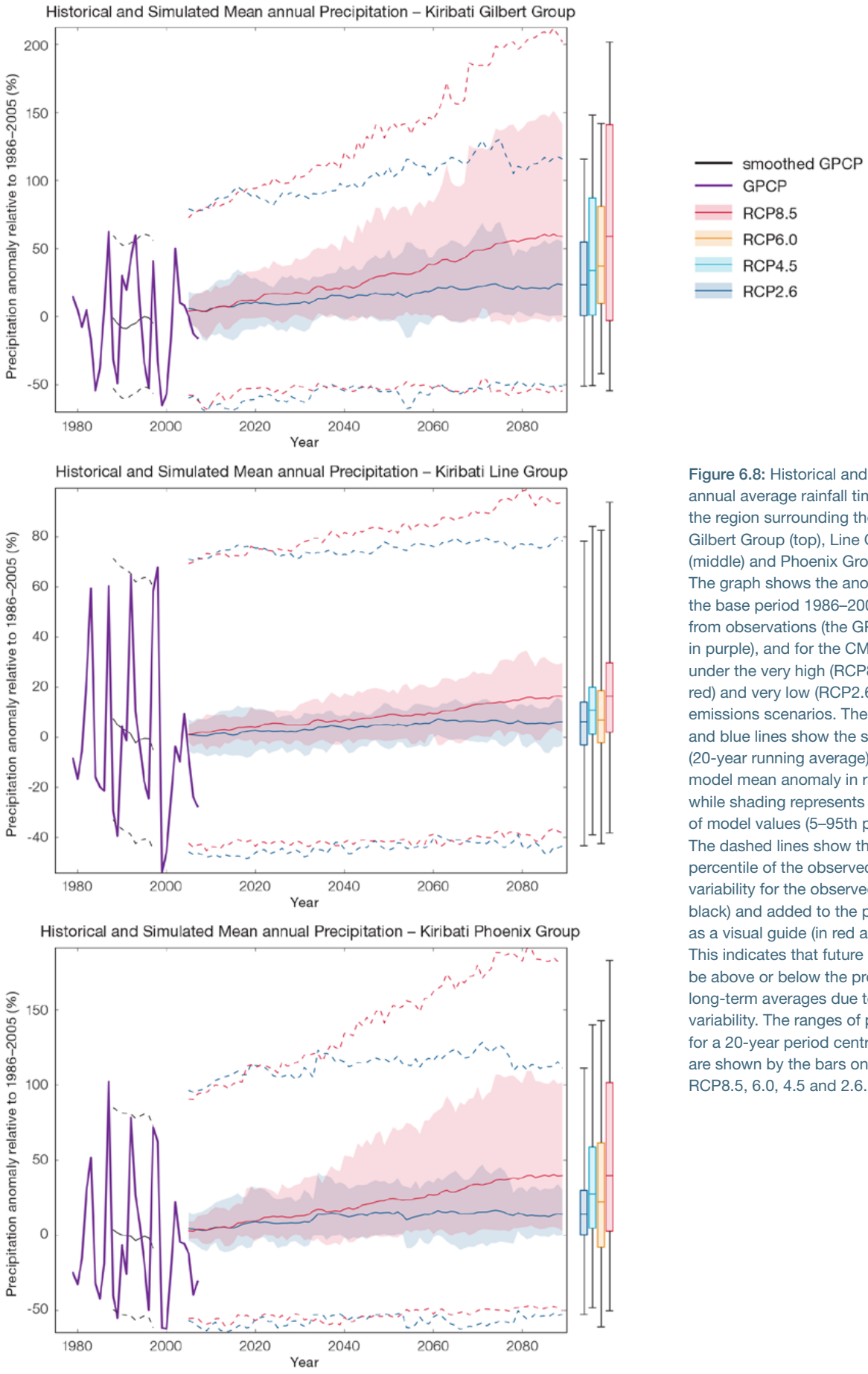

Figure 6.8: Historical and simulated annual average rainfall time series for the region surrounding the Kiribati Gilbert Group (top), Line Group (middle) and Phoenix Group (bottom). The graph shows the anomaly (from the base period 1986–2005) in rainfall from observations (the GPCP dataset, in purple), and for the CMIP5 models under the very high (RCP8.5, in red) and very low (RCP2.6, in blue) emissions scenarios. The solid red and blue lines show the smoothed (20-year running average) multi-model mean anomaly in rainfall, while shading represents the spread of model values (5–95th percentile). The dashed lines show the 5–95th percentile of the observed interannual variability for the observed period (in black) and added to the projections as a visual guide (in red and blue). This indicates that future rainfall could be above or below the projected long-term averages due to interannual variability. The ranges of projections for a 20-year period centred on 2090 are shown by the bars on the right for RCP8.5, 6.0, 4.5 and 2.6.

There is general agreement between models that rainfall will increase. However there are important biases in the models in the region, which lowers the confidence of the projected changes and makes the amount difficult to determine. The 5–95th percentile range of projected values from CMIP5 climate models is large, for example in the Phoenix Group for RCP8.5 the range is 1–34% by 2030 and 3 to +102% by 2090.

There is *high confidence* that the long-term rainfall over Kiribati will increase because:

- The majority of CMIP3 and CMIP5 models indicate that rainfall will increase along the equator, however confidence in the magnitude of this change is influenced by the 'cold-tongue bias' in the current climate (Chapter 1);
- The majority of models agree that the rainfall in the ITCZ will increase under a warmer climate; and
- Changes in the SPCZ rainfall are uncertain. The majority of CMIP5 models simulate increased rainfall in the western part of the SPCZ (Brown et al., 2013a) and decreased rainfall in the eastern part of the SPCZ, however rainfall changes are sensitive to sea-surface temperature gradients, which are not well simulated in many models (Widlansky et al., 2013). See Box in Chapter 1 for more details.

There is *low confidence* in the model average rainfall change shown in Tables 6.5–6.7 because:

- The complex set of processes involved in tropical rainfall is challenging to simulate in models. This means that the confidence in the projection of rainfall is generally lower than for other variables such as temperature;
- The CMIP5 models (similar to the previous CMIP3 models) have a bias in the present day average rainfall of Kiribati due to the 'cold-tongue bias' (Chapter 1), and biases in the ITCZ and the SPCZ;
- There is a different magnitude of rainfall change in the SPCZ projected by models that have reduced sea-surface temperature biases (Australian Bureau of Meteorology and CSIRO, 2011, Chapter 7 (downscaling); Widlanksy et al., 2012) compared to the CMIP5 models; and
- The future behaviour of the ENSO is unclear, and the ENSO strongly influences year-to-year rainfall variability.

6.5.3 Extremes

Extreme Temperature

The temperature on extremely hot days is projected to increase by about the same amount as average temperature. This conclusion is based on analysis of daily temperature data from a subset of CMIP5 models (Chapter 1). The frequency of extremely hot days is also expected to increase.

For the Gilbert Islands the temperature of the 1-in-20-year hot day is projected to increase by approximately 0.6°C by 2030 under the RCP2.6 (very low) scenario and by 0.9°C under the RCP8.5 (very high) scenario. By 2090 the projected increase is 0.8°C for RCP2.6 (very low) and 3°C for RCP8.5 (very high).

For the Phoenix Islands the temperature of the 1-in-20-year hot day is projected to increase by approximately 0.6°C by 2030 under the RCP2.6 (very low) scenario and by 0.8°C under the RCP8.5 (very high) scenario. By 2090 the projected increase is 0.8°C for RCP2.6 (very low) and 3°C for RCP8.5 (very high).

For the Line Islands the temperature of the 1-in-20-year hot day is projected to increase by approximately 0.7°C by 2030 under the RCP2.6 (very low) scenario and by 0.9°C under the RCP8.5 (very high) scenario. By 2090 the projected increase is 0.8°C for RCP2.6 (very low) and 3°C for RCP8.5 (very high).

There is *very high confidence* that the temperature of extremely hot days and the temperature of extremely cool days will increase, because:

- A change in the range of temperatures, including the extremes, is physically consistent with rising greenhouse gas concentrations;
- This is consistent with observed changes in extreme temperatures around the world over recent decades; and
- All the CMIP5 models agree on an increase in the frequency and intensity of extremely hot days and a decrease in the frequency and intensity of cool days.

There is *low confidence* in the magnitude of projected change in extreme temperature because models generally underestimate the current intensity and frequency of extreme events, especially in this area, due to the 'cold-tongue bias' (Chapter 1). Changes to the particular driver of extreme temperatures affect whether the change to extremes is more or less than the change in the average temperature, and the changes to the drivers of extreme temperatures in Kiribati are currently unclear. Also, while all models project the same direction of change there is a wide range in the projected magnitude of change among the models.

Extreme Rainfall

The frequency and intensity of extreme rainfall events are projected to increase. This conclusion is based on analysis of daily rainfall data from a subset of CMIP5 models using a similar method to that in Australian Bureau of Meteorology and CSIRO (2011) with some improvements (Chapter 1), so the results are slightly different to those in Australian Bureau of Meteorology and CSIRO (2011).

For the Gilbert Islands the current 1-in-20-year daily rainfall amount is projected to increase by approximately 6 mm by 2030 for RCP2.6 and by 8 mm by 2030 for RCP8.5 (very high emissions). By 2090, it is projected to increase by approximately 13 mm for RCP2.6 and by 30 mm for RCP8.5 (very high emissions).The majority of models project the current 1-in-20-year daily rainfall event will become, on average, a 1-in-7-year event for RCP2.6 and a 1-in-5-year event for RCP8.5 (very high emissions) by 2090.

For the Phoenix Islands the current 1-in-20-year daily rainfall amount is projected to increase by approximately 9 mm by 2030 for RCP2.6 and by 6 mm by 2030 for RCP8.5 (very high emissions). By 2090, it is projected to increase by approximately 12 mm for RCP2.6 and by 36 mm for RCP8.5 (very high emissions).The majority of models project the current 1-in-20-year daily rainfall event will become, on average, a 1-in-7-year event for RCP2.6 and a 1-in-5-year event for RCP8.5 (very high emissions) by 2090.

For the Line Islands the current 1-in-20-year daily rainfall amount is projected to increase by approximately 7 mm by 2030 for RCP2.6 and by 8 mm by 2030 for RCP8.5 (very high emissions). By 2090, it is projected to increase by approximately 8 mm for RCP2.6 and by 42 mm for RCP8.5 (very high emissions).The majority of models project the current 1-in-20-year daily rainfall event will become, on average, a 1-in-8-year event for RCP2.6 and a 1-in-4-year event for RCP8.5 (very high emissions) by 2090. These results are different to those found in Australian Bureau of Meteorology and CSIRO (2011) because of different methods used (Chapter 1).

There is *high confidence* that the frequency and intensity of extreme rainfall events will increase because:

- A warmer atmosphere can hold more moisture, so there is greater potential for extreme rainfall (IPCC, 2012); and
- Increases in extreme rainfall in the Pacific are projected in all available climate models.

There is *low confidence* in the magnitude of projected change in extreme rainfall because:

- Models generally underestimate the current intensity of local extreme events, especially in this area due to the 'cold-tongue bias' (Chapter 1);
- Changes in extreme rainfall projected by models may be underestimated because models seem to underestimate the observed increase in heavy rainfall with warming (Min et al., 2011);
- GCMs have a coarse spatial resolution, so they do not adequately capture some of the processes involved in extreme rainfall events; and
- The Conformal Cubic Atmospheric Model (CCAM) downscaling model has finer spatial resolution and the CCAM results presented in Australian Bureau of Meteorology and CSIRO (2011) indicates a smaller increase in the number of extreme rainfall days, and there is no clear reason to accept one set of models over another.

Drought

Drought projections (defined in Chapter 1) are described in terms of changes in proportion of time in drought, frequency and duration by 2090 for very low and very high emissions (RCP2.6 and 8.5).

For the Gilbert Islands the overall proportion of time spent in drought is expected to decrease under all scenarios. Under RCP8.5 the frequency of mild, moderate and severe drought is projected to decrease while the frequency of extreme drought is projected to remain stable. The duration of events in all drought categories is projected to stay approximately the same under RCP8.5 (Figure 6.9). Under RCP2.6 (very low emissions) the frequency of mild, moderate and severe drought is projected to decrease while the frequency of extreme drought is projected to remain stable. The duration of events in all categories is projected to stay approximately the same under RCP2.6 (very low emissions).

For the Phoenix Islands the overall proportion of time spent in drought is expected to decrease under all scenarios. Under RCP8.5 the frequency of mild, moderate and severe drought is projected to decrease while the frequency of extreme drought is projected to remain stable. The duration of events in all drought categories is projected to stay approximately the same under RCP8.5. Under RCP2.6 (very low emissions) the frequency of mild, moderate and severe drought is projected to decrease while the frequency of extreme drought is projected to remain stable. The duration of events in all categories is projected to stay approximately the same under RCP2.6 (very low emissions).

For the Line Islands the overall proportion of time spent in drought is expected to decrease under all scenarios. Under RCP8.5 the frequency of mild, moderate and severe drought is projected to decrease while the frequency of extreme drought is projected to remain stable. The duration of extreme drought events is projected to increase slightly while in all other drought categories is projected to stay approximately the same under RCP8.5. Under RCP2.6 (very low emissions) the frequency of mild, moderate and severe drought is projected to decrease while the frequency of extreme drought is projected to remain stable. The duration of events in all categories is projected to stay approximately the same under RCP2.6 (very low emissions).

There is *medium confidence* in this direction of change because:

- There is only *medium confidence* in the direction of mean rainfall change;
- These drought projections are based upon a subset of models; and
- Like the CMIP3 models, the majority of the CMIP5 models agree on this direction of change.

There is *low confidence* in the projections of drought frequency and duration because there is *low confidence* in the magnitude of rainfall projections, and no consensus about projected changes in the ENSO, which directly influence the projection of drought.

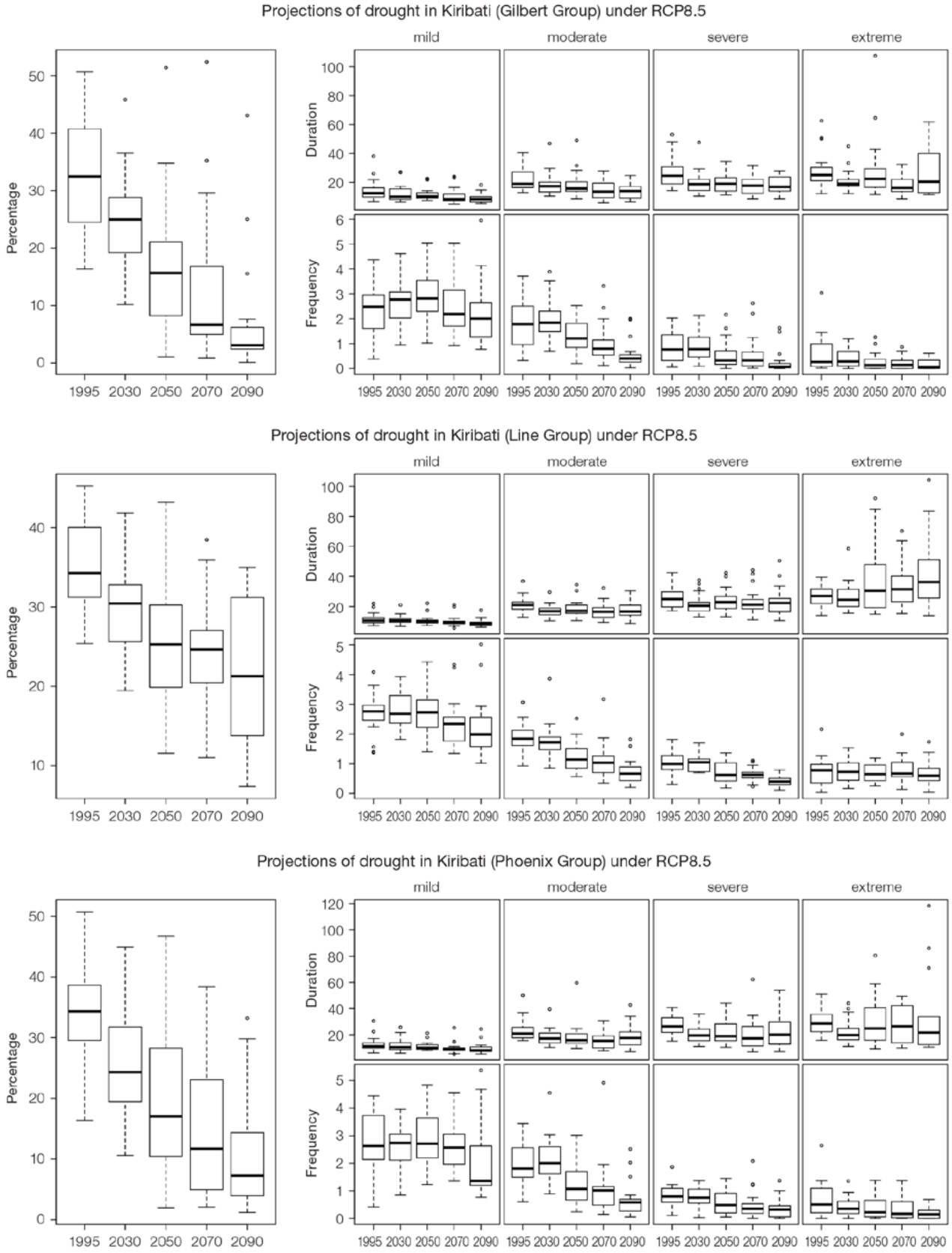

Figure 6.9: Box-plots showing percent of time in moderate, severe or extreme drought (left hand side), and average drought duration and frequency for the different categories of drought (mild, moderate, severe and extreme) for the Kiribati Gilbert Group (top), Line group (middle) and Phoenix group (bottom). These are shown for 20-year periods centred on 1995, 2030, 2050, 2070 and 2090 for the RCP8.5 (very high emissions) scenario. The thick dark lines show the median of all models, the box shows the interquartile (25–75%) range, the dashed lines show 1.5 times the interquartile range and circles show outlier results.

6.5.4 Coral Reefs and Ocean Acidification

As atmospheric CO_2 concentrations continue to rise, oceans will warm and continue to acidify. These changes will impact the health and viability of marine ecosystems, including coral reefs that provide many key ecosystem services (*high confidence).* These impacts are also likely to be compounded by other stressors such as storm damage, fishing pressure and other human impacts.

The projections for future ocean acidification and coral bleaching use three RCPs (2.6, 4.5, and 8.5).

Ocean Acidification

Ocean acidification is expressed in terms of aragonite saturation state (Chapter 1). In Kiribati, the aragonite saturation state has declined from about 4.5 in the late 18th century to an observed value of about 3.9±0.1 by 2000 (Kuchinke et al., 2014). All models show that the aragonite saturation state, a proxy for coral reef growth rate, will continue to decrease as atmospheric CO_2 concentrations increase (*very high confidence*).

Projections from CMIP5 models indicate that under RCPs 8.5 (very high emissions) and 4.5 (low emissions) the median aragonite saturation state will transition to marginal conditions (3.5) around 2030. In RCP8.5 (very high emissions) the aragonite saturation state continues to strongly decline thereafter to values where coral reefs have not historically been found (< 3.0). Under RCP4.5 (low emissions) the aragonite saturation plateaus around 3.2 i.e. marginal conditions for healthy coral reefs.

While under RCP2.6 (very low emissions) the median aragonite saturation state never falls below 3.5 in the Gilbert and Phoenix Islands, and increases slightly toward the end of the century (Figure 6.10) suggesting that the conditions remains adequate for healthy corals reefs. However in the Line Islands the median aragonite saturation state falls below 3.5 and settles at a value of ~3.4 by the end of this century. There is *medium confidence* in this range and distribution of possible futures because the projections are based on climate models that do not resolve the reef scale that can play a role in modulating large-scale changes. The impacts of ocean acidification are also likely to affect the entire marine ecosystem impacting the key ecosystem services provided by reefs.

Coral Bleaching Risk

As the ocean warms, the risk of coral bleaching increases (*very high confidence*). There is *medium confidence* in the projected rate of change for Kiribati because there is *medium confidence* in the rate of change of sea-surface temperature (SST), and the changes at the reef scale (which can play a role in modulating large-scale changes) are not adequately resolved. Importantly, the coral bleaching risk calculation does not account the impact of other potential stressors (Chapter 1).

The changes in the frequency (or recurrence) and duration of severe bleaching risk are quantified for different projected SST changes (Table 6.4). Overall there is a decrease in the time between two periods of elevated risk and an increase in the duration of the elevated risk. For example, under a long-term mean increase of 1°C (relative to 1982–1999 period), the average period of severe bleaching risk (referred to as a risk event) will last 4.7 months (with a minimum duration of 2.3 weeks and a maximum duration of 12.0 months) and the average time between two risks will be 1.2 years (with the minimum recurrence of 1.2 months and a maximum recurrence of 4.2 years). If severe bleaching events occur more often than once every five years, the long-term viability of coral reef ecosystems becomes threatened.

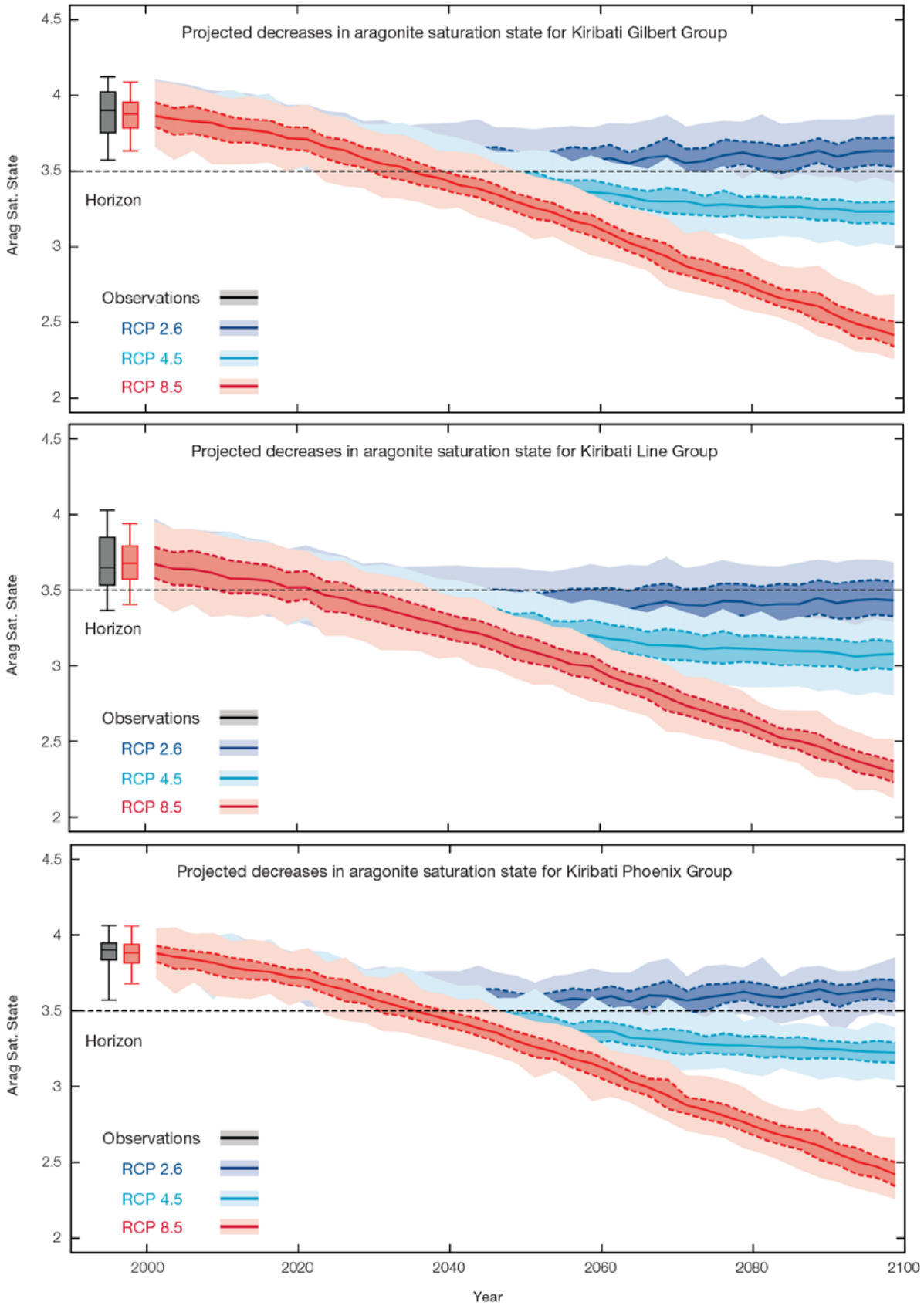

Figure 6.10: Projected decreases in aragonite saturation state in the three island groups of Kiribati, Gilbert Group (upper), the Line Group (middle) and the Phoenix Group (lower) from CMIP5 under RCPs 2.6, 4.5 and 8.5. Shown are the median values (solid line), the interquartile range (dashed lines), and 5% and 95% percentiles (light shading). The horizontal line represents the transition to marginal conditions for coral reef health (from Guinotte et al., 2003).

Table 6.4: Projected changes in severe coral bleaching risk for the Kirabati EEZ for increases in SST relative to 1982–1999.

Temperature change [1]	Recurrence interval [2]	Duration of the risk event [3]
Change in observed mean	11.8 years (8.0 years – 16.5 years)	10.5 weeks (4.9 weeks – 17.9 weeks)
+0.25°C	9.6 years (5.9 years – 14.3 years)	12.0 weeks (4.5 weeks – 5.1 months)
+0.5°C	7.5 years (4.4 years – 12.1 years)	12.4 weeks (3.3 weeks – 6.2 months)
+0.75°C	2.5 years (3.7 months – 6.7 years)	3.4 months (2.3 weeks – 8.5 months)
+1°C	1.2 years (1.2 months – 4.2 years)	4.7 months (2.3 weeks –12.0 months)
+1.5°C	8.4 months (0.9 months – 2.3 years)	8.1 months (2.9 weeks – 2.5 years)
+2°C	4.7 months (1.0 months – 11.8 months)	9.7 months (4.4 weeks – 5.5 years)

[1] This refers to projected SST anomalies above the mean for 1982–1999.
[2] Recurrence is the mean time between severe coral bleaching risk events. Range (min – max) shown in brackets.
[3] Duration refers to the period of time where coral are exposed to the risk of severe bleaching Range (min – max) shown in brackets.

6.5.5 Sea Level

Mean sea level is projected to continue to rise over the course of the 21st century. There is very *high confidence* in the direction of change. The CMIP5 models simulate a rise of between approximately 7–17 cm by 2030 (very similar values for different RCPs), with increases of 38–87 cm by 2090 under the RCP8.5 (Figure 6.11 and Tables 6.5-6.7). There is *medium confidence* in the range mainly because there is still uncertainty associated with projections of the Antarctic ice sheet contribution. Interannual variability of sea level will lead to periods of lower and higher regional sea levels. In the past, this interannual variability has been about 23 cm (5–95% range, after removal of the seasonal signal, see dashed lines in Figure 6.11 (a) and it is likely that a similar range will continue through the 21st century.

6.5.6 Wind-driven Waves

The projected changes in wave climate vary across Kiribati.

In the Gilbert Islands, there is a projected decrease in November–April wave height (significant in February and March in 2035 under RCP8.5 (very high emissions) and in 2090 under both RCP4.5 and RCP8.5, and significant in February only in 2035 under RCP4.5) (Figure 6.12) accompanied by a suggested decrease in wave period (significant in some months by 2090), with no change in direction *(low confidence)* (Table 6.8). In May–October there is no projected change in wave height or period, but a clockwise rotation is projected toward the South (significant in October in 2035 under RCP4.5 and in 2090 under both RCP4.5 and RCP8.5 (very high emissions) *(low confidence)*. A decrease of about 20 cm in the height of storm waves is suggested in December–March *(low confidence)*.

In the Phoenix Islands, there is a projected decrease in November–March wave height (significant in February in 2035 and 2090 under RCP8.5) (Figure 6.13) with no significant change in wave period or direction *(low confidence)* (Table 6.9). In June–September there is no projected change in wave height or period, with a clockwise rotation toward the South suggested (significant in October in 2090 under RCP8.5*, very high confidence*) *(low confidence)*. No change in storm wave properties is projected *(low confidence)*.

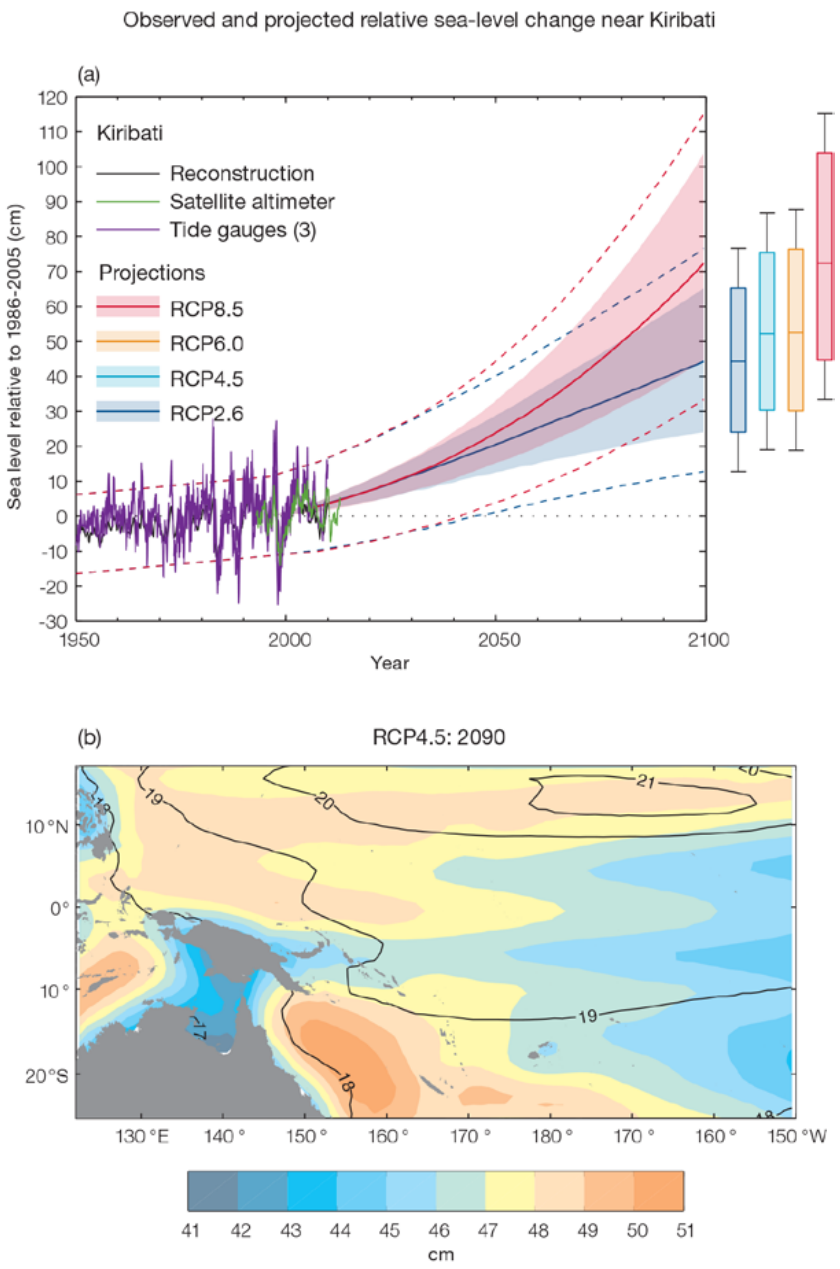

Figure 6.11: (a) The observed tide-gauge records of relative sea-level (since the late 1970s) are indicated in purple, and the satellite record (since 1993) in green. The gridded (reconstructed) sea level data at Kiribati (since 1950) is shown in black. Multi-model mean projections from 1995–2100 are given for the RCP8.5 (red solid line) and RCP2.6 emissions scenarios (blue solid line), with the 5–95% uncertainty range shown by the red and blue shaded regions. The ranges of projections for four emission scenarios (RCPs 2.6, 4.5, 6.0 and 8.5) by 2100 are also shown by the bars on the right. The dashed lines are an estimate of interannual variability in sea level (5–95% uncertainty range about the projections) and indicate that individual monthly averages of sea level can be above or below longer-term averages.

(b) The regional distribution of projected sea level rise under the RCP4.5 emissions scenario for 2081–2100 relative to 1986–2005. Mean projected changes are indicated by the shading, and the estimated uncertainty in the projections is indicated by the contours (in cm).

In the Line Islands, projected changes in wave properties include a small decrease in wave height (significant in February under RCP8.5, very high emissions, in 2035) (Figure 6.14), with a possible small decrease in wave period and no change in direction during December–March *(low confidence)* (Table 6.10), though there is a suggestion of less north-easterly waves with more waves from the north and the east. During June–September, wave height is projected to increase slightly in September (significant in 2090 under both RCP4.5 and RCP8.5, very high emissions), with no projected change in wave period or direction *(low confidence)*. No change in storm wave properties is projected *(low confidence)*.

There is *low confidence* in projected changes in the Kiribati wind-wave climate because:

- Projected changes in wave climate are dependent on confidence in projected changes in the ENSO, which is low; and
- The differences between simulated and observed (hindcast) wave data are larger than the projected wave changes, which further reduces our confidence in projections.

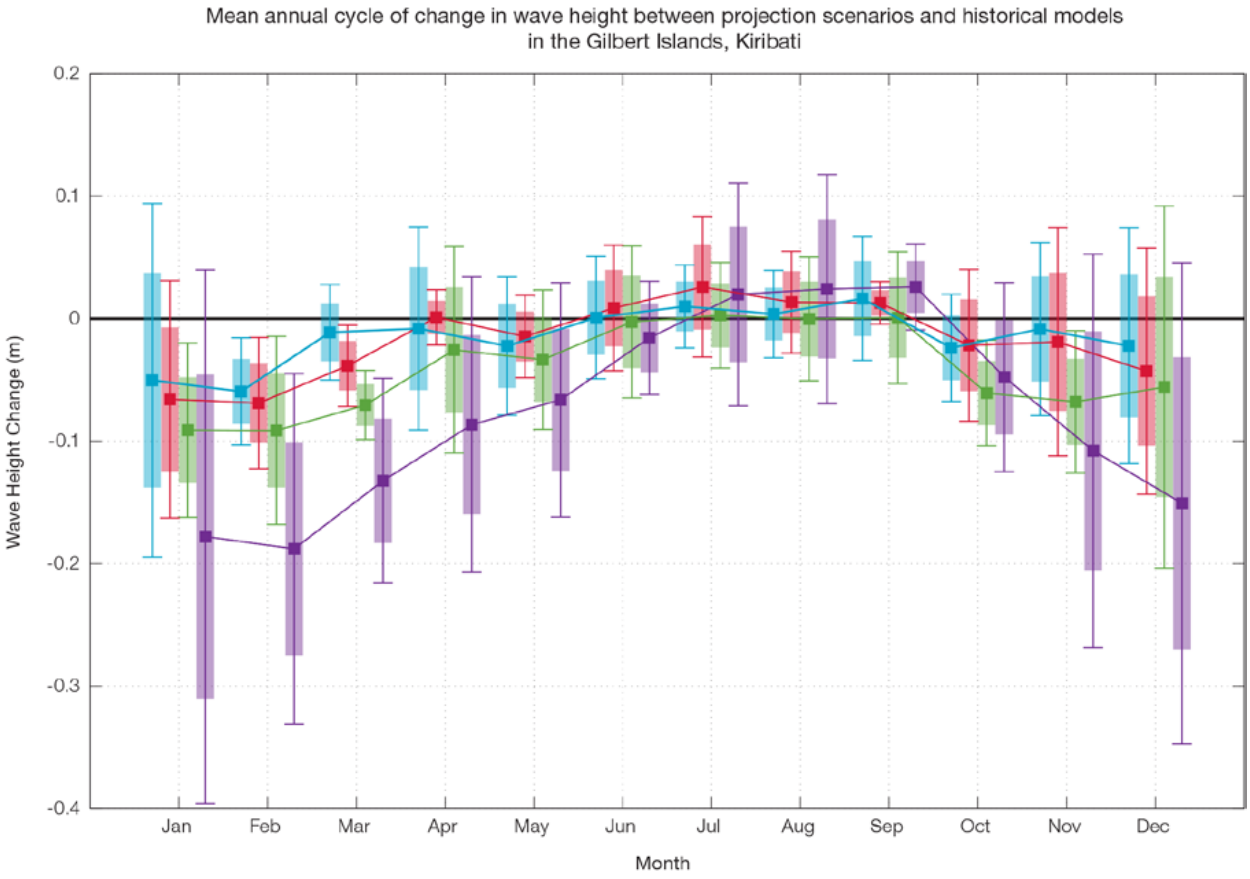

Figure 6.12: Mean annual cycle of change in wave height between projection scenarios and historical models in the Gilbert Islands, Kiribati. This plot shows a decrease in wave heights in the northern trade winds season (December–March) (significant in February in all projections), and no change in the southern trade winds months of June–September. Shaded boxes show 1 standard deviation of models' means around the ensemble means, and error bars show the 5–95% range inferred from the standard deviation. Colours represent RCP scenarios and time periods: blue 2035 RCP4.5 (low emissions), red 2035 RCP8.5 (very high emissions), green 2090 RCP4.5 (low emissions), purple 2090 RCP8.5 (very high emissions).

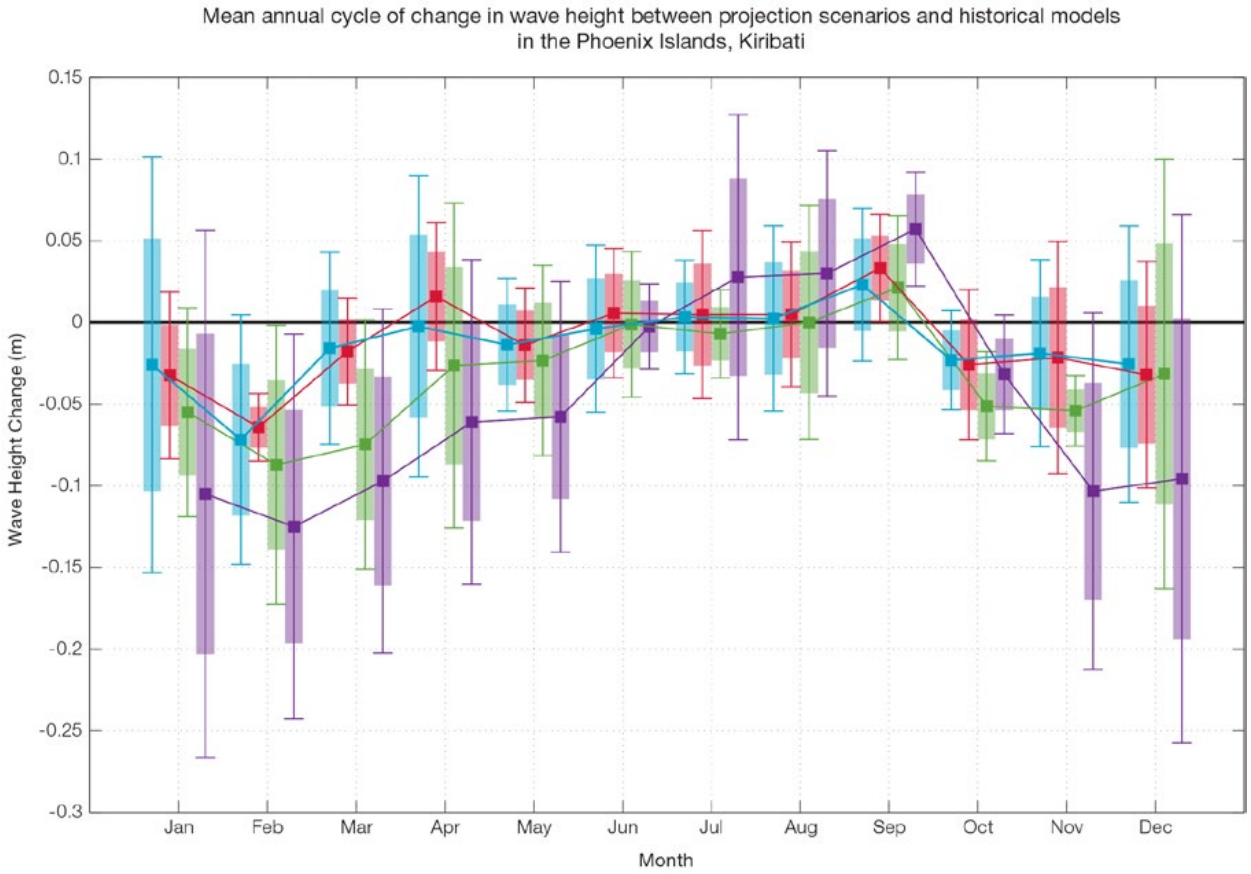

Figure 6.13: Mean annual cycle of change in wave height between projection scenarios and historical models in the Phoenix Islands, Kiribati. This plot shows a decrease in wave heights in the northern trade wind season (December–March) (significant in February under RCP4.5 and RCP8.5, very high emissions, in 2090, as well as RCP8.5, very high emissions, in 2035), and no significant change in June–September (though a significant increase in wave height is projected under RCP8.5, very high emissions, in 2090). Shaded boxes show 1 standard deviation of models' means around the ensemble means, and error bars show the 5–95% range inferred from the standard deviation. Colours represent RCP scenarios and time periods: blue 2035 RCP4.5 (low emissions), red 2035 RCP8.5 (very high emissions), green 2090 RCP4.5 (low emissions), purple 2090 RCP8.5 (very high emissions).

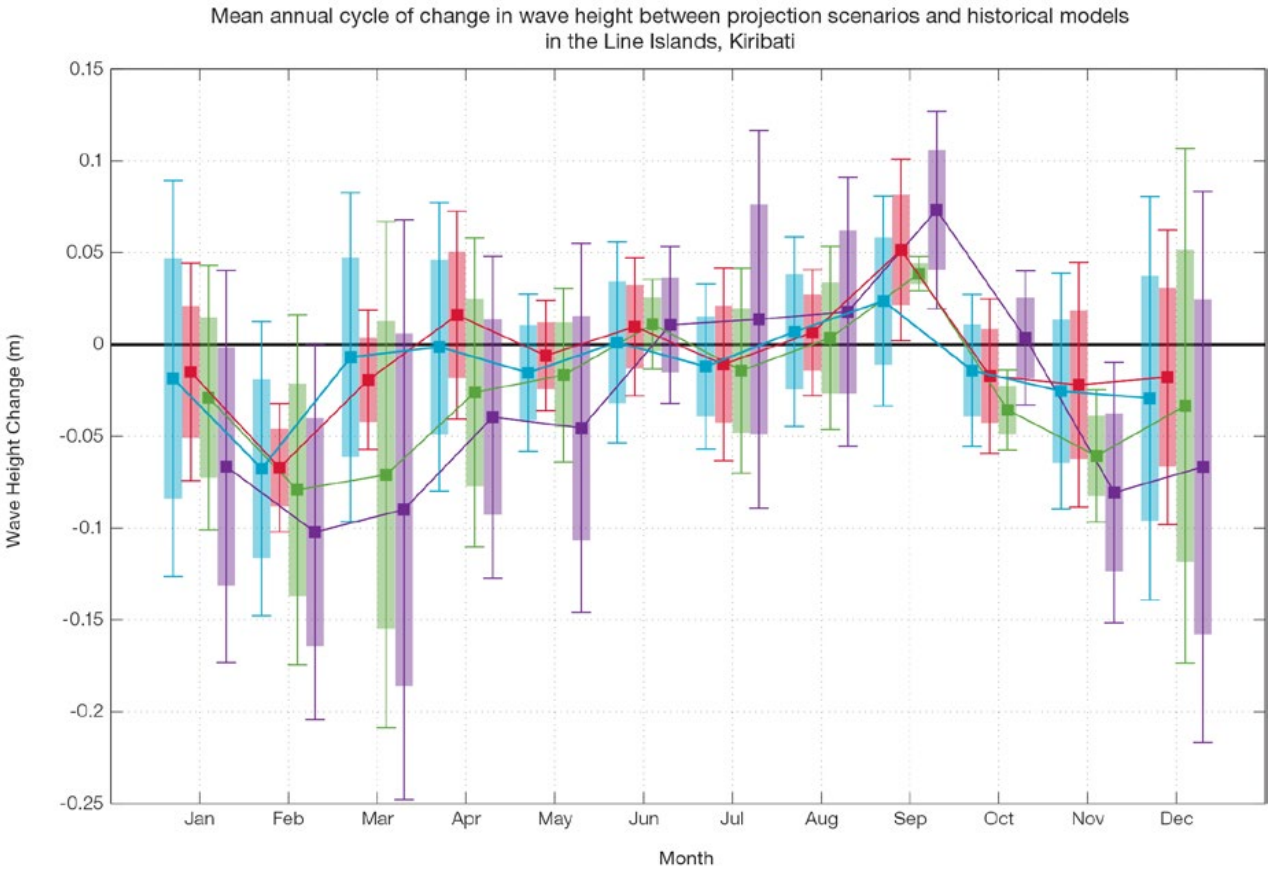

Figure 6.14: Mean annual cycle of change in wave height between projection scenarios and historical models in the Line Islands, Kiribati. This plot shows a decrease in wave heights in November–March (significant under RCP8.5 (very high emissions) in 2090 in November and February, as well as RCP4.5 2090 in November and RCP8.5, very high emissions, 2035 in February), and no significant change in June-August, with an increase in height significant in September in 2090. Shaded boxes show 1 standard deviation of models' means around the ensemble means, and error bars show the 5–95% range inferred from the standard deviation. Colours represent RCP scenarios and time periods: blue 2035 RCP4.5 (low emissions), red 2035 RCP8.5 (very high emissions), green 2090 RCP4.5 (low emissions), purple 2090 RCP8.5 (very high emissions).

6.5.7 Projections Summary

There is *very high confidence* in the direction of long-term change in a number of key climate variables, namely an increase in mean and extremely high temperatures, sea level and ocean acidification. There is *high confidence* that the frequency and intensity of extreme rainfall will increase. There is *medium confidence* that mean rainfall will increase, and *medium confidence* in a decrease in drought frequency.

Tables 6.5–6.10 quantify the mean changes and ranges of uncertainty for a number of variables, years and emissions scenarios. A number of factors are considered in assessing confidence, i.e. the type, amount, quality and consistency of evidence (e.g. mechanistic understanding, theory, data, models, expert judgment) and the degree of agreement, following the IPCC guidelines (Mastrandrea et al., 2010). Confidence ratings in the projected magnitude of mean change are generally lower than those for the direction of change (see paragraph above) because magnitude of change is more difficult to assess. For example, there is *very high confidence* that temperature will increase, but *medium confidence* in the magnitude of mean change.

Table 6.5: Projected changes in the annual and seasonal mean climate for Kiribati Gilbert Group under four emissions scenarios; RCP2.6 (very low emissions, in dark blue), RCP4.5 (low emissions, in light blue), RCP6 (medium emissions, in orange) and RCP8.5 (very high emissions, in red). Projected changes are given for four 20-year periods centred on 2030, 2050, 2070 and 2090, relative to a 20-year period centred on 1995. Values represent the multi-model mean change, with the 5–95% range of uncertainty in brackets. Confidence in the magnitude of change is expressed as *high*, *medium* or *low*. Surface air temperatures in the Pacific are closely related to sea-surface temperatures (SST), so the projected changes to air temperature given in this table can be used as a guide to the expected changes to SST. (See also Section 1.5.2). 'NA' indicates where data are not available.

Variable	Season	2030	2050	2070	2090	Confidence (magnitude of change)
Surface air temperature (°C)	Annual	0.7 (0.4–1)	0.9 (0.6–1.5)	0.9 (0.5–1.4)	0.9 (0.6–1.5)	*Medium*
		0.8 (0.4–1.2)	1.1 (0.6–1.7)	1.4 (0.8–2.1)	1.6 (1.1–2.5)	
		0.7 (0.4–1)	1 (0.7–1.6)	1.5 (0.9–2.3)	1.9 (1.1–2.9)	
		0.9 (0.6–1.2)	1.5 (1–2.2)	2.3 (1.5–3.5)	3.1 (2.1–4.5)	
Maximum temperature (°C)	1-in-20 year event	0.6 (0.2–1.1)	0.7 (0.3–1.2)	0.8 (0.3–1.4)	0.8 (0.4–1.3)	*Medium*
		0.7 (0.2–0.9)	0.9 (0.5–1.2)	1.2 (0.6–1.9)	1.3 (0.9–2.2)	
		NA (NA–NA)	NA (NA–NA)	NA (NA–NA)	NA (NA–NA)	
		0.9 (0.2–1.4)	1.5 (0.8–2.3)	2.3 (1.2–3.4)	2.9 (1.8–4.4)	
Minimum temperature (°C)	1-in-20 year event	0.7 (0.3–0.9)	0.8 (0.4–1.5)	0.9 (0.2–1.5)	0.9 (0.4–1.2)	*Medium*
		0.6 (0.3–1)	1 (0.6–1.4)	1.2 (0.7–2)	1.4 (1–2)	
		NA (NA–NA)	NA (NA–NA)	NA (NA–NA)	NA (NA–NA)	
		0.9 (0.3–1.3)	1.6 (0.9–2.6)	2.5 (1.6–3.9)	3.1 (2.1–4.4)	
Total rainfall (%)	Annual	10 (-9–27)	16 (-3–44)	21 (-1–59)	24 (1–55)	*Low*
		16 (0–37)	21 (1–72)	29 (-1–74)	34 (1–87)	
		16 (1–37)	22 (1–43)	25 (4–60)	37 (10–81)	
		18 (2–43)	30 (-2–70)	48 (-4–124)	59 (-3–141)	
Total rainfall (%)	Nov-Apr	5 (-21–21)	13 (-12–37)	17 (-5–52)	21 (-8–49)	*Low*
		13 (-8–36)	17 (-8–61)	23 (-5–69)	23 (-11–77)	
		16 (-1–34)	21 (-2–45)	20 (-4–53)	29 (-4–84)	
		12 (-7–27)	25 (-7–73)	34 (-8–107)	42 (-8–128)	
Total rainfall (%)	May-Oct	15 (1–37)	20 (2–50)	25 (-8–69)	25 (5–58)	*Low*
		18 (-2–44)	26 (-1–71)	36 (3–101)	44 (11–110)	
		14 (-3–40)	23 (-7–51)	30 (-1–69)	46 (11–83)	
		24 (5–58)	36 (7–87)	64 (10–155)	78 (7–169)	
Aragonite saturation state (Ωar)	Annual	-0.3 (-0.6–-0.1)	-0.4 (-0.7–-0.1)	-0.4 (-0.6–-0.1)	-0.3 (-0.6–-0.1)	*Medium*
		-0.3 (-0.6–0.0)	-0.5 (-0.7–-0.2)	-0.6 (-0.9–-0.4)	-0.7 (-0.9–-0.4)	
		NA (NA–NA)	NA (NA–NA)	NA (NA–NA)	NA (NA–NA)	
		-0.3 (-0.6–-0.1)	-0.6 (-0.9–-0.4)	-1.0 (-1.2–-0.7)	-1.3 (-1.6–-1.1)	
Mean sea level (cm)	Annual	12 (7–17)	21 (13–29)	31 (18–44)	40 (23–59)	*Medium*
		12 (7–16)	22 (13–30)	33 (20–47)	46 (27–66)	
		11 (7–16)	21 (13–29)	33 (19–46)	47 (28–67)	
		12 (7–17)	24 (16–33)	40 (26–56)	61 (38–87)	

Table 6.6: Projected changes in the annual and seasonal mean climate for Kiribati Phoenix Group under four emissions scenarios; RCP2.6 (very low emissions, in dark blue), RCP4.5 (low emissions, in light blue), RCP6 (medium emissions, in orange) and RCP8.5 (very high emissions, in red). Projected changes are given for four 20-year periods centred on 2030, 2050, 2070 and 2090, relative to a 20-year period centred on 1995. Values represent the multi-model mean change, with the 5–95% range of uncertainty in brackets. Confidence in the magnitude of change is expressed as *high*, *medium* or *low*. Surface air temperatures in the Pacific are closely related to sea-surface temperatures (SST), so the projected changes to air temperature given in this table can be used as a guide to the expected changes to SST. (See also Section 1.5.2). 'NA' indicates where data are not available.

Variable	Season	2030	2050	2070	2090	Confidence (magnitude of change)
Surface air temperature (°C)	Annual	0.7 (0.5–1)	0.9 (0.6–1.4)	0.9 (0.5–1.4)	0.9 (0.6–1.4)	*Medium*
		0.7 (0.4–1.1)	1.1 (0.7–1.7)	1.4 (0.8–2.1)	1.6 (1–2.4)	
		0.7 (0.4–1)	1 (0.6–1.5)	1.4 (0.9–2.1)	1.8 (1.1–2.8)	
		0.9 (0.5–1.2)	1.5 (0.9–2.2)	2.3 (1.6–3.4)	3 (2.1–4.3)	
Maximum temperature (°C)	1-in-20 year event	0.6 (-0.2–1)	0.9 (0.4–1.4)	0.7 (-0.3–1.4)	0.8 (-0.1–1.4)	*Medium*
		0.7 (0–1.1)	0.9 (0.2–1.4)	1.2 (0.2–1.9)	1.4 (0.7–2.3)	
		NA (NA–NA)	NA (NA–NA)	NA (NA–NA)	NA (NA–NA)	
		0.8 (-0.1–1.3)	1.4 (0.5–2.1)	2.3 (0.7–3.4)	3 (1.3–4.4)	
Minimum temperature (°C)	1-in-20 year event	0.6 (0.1–0.9)	0.8 (0.4–1.1)	0.8 (0.3–1.4)	0.8 (0.2–1.4)	*Medium*
		0.6 (0.2–0.9)	1 (0.6–1.3)	1.2 (0.7–1.8)	1.4 (0.7–1.9)	
		NA (NA–NA)	NA (NA–NA)	NA (NA–NA)	NA (NA–NA)	
		0.8 (0.4–1.4)	1.5 (0.9–2.3)	2.4 (1.6–3.5)	3.1 (2–4.2)	
Total rainfall (%)	Annual	8 (-4–22)	15 (1–36)	15 (-8–40)	14 (0–30)	*Low*
		12 (-4–33)	15 (-3–49)	21 (1–61)	27 (5–59)	
		12 (-1–33)	14 (-4–31)	16 (-8–48)	22 (-8–61)	
		13 (1–34)	23 (-1–60)	34 (1–92)	40 (3–102)	
Total rainfall (%)	Nov-Apr	10 (-8–29)	21 (-1–52)	20 (-9–60)	20 (1–41)	*Low*
		18 (-11–52)	22 (-5–82)	29 (0–88)	35 (9–74)	
		17 (2–41)	22 (3–50)	22 (-9–58)	34 (-8–91)	
		18 (-2–56)	34 (-1–116)	49 (5–147)	54 (3–148)	
Total rainfall (%)	May-Oct	6 (-6–17)	11 (1–22)	10 (-7–29)	9 (-5–25)	*Low*
		9 (-6–25)	9 (-5–27)	15 (-4–39)	20 (2–44)	
		7 (-6–26)	8 (-8–20)	11 (-8–34)	14 (-8–38)	
		9 (-2–23)	16 (-2–40)	23 (-1–59)	29 (2–68)	
Aragonite saturation state (Ωar)	Annual	-0.3 (-0.6–-0.1)	-0.4 (-0.6–-0.1)	-0.4 (-0.6–-0.1)	-0.3 (-0.6–-0.1)	*Medium*
		-0.3 (-0.6–0.0)	-0.5 (-0.7–-0.2)	-0.6 (-0.9–-0.4)	-0.7 (-0.9–-0.4)	
		NA (NA–NA)	NA (NA–NA)	NA (NA–NA)	NA (NA–NA)	
		-0.3 (-0.6–-0.1)	-0.6 (-0.9–-0.4)	-1.0 (-1.2–-0.7)	-1.3 (-1.6–-1.1)	
Mean sea level (cm)	Annual	12 (7–17)	21 (13–29)	31 (18–44)	40 (23–59)	*Medium*
		12 (7–16)	22 (13–30)	33 (20–47)	46 (27–66)	
		11 (7–16)	21 (13–29)	33 (19–46)	47 (28–67)	
		12 (7–17)	24 (16–33)	40 (26–56)	61 (38–87)	

Table 6.7: Projected changes in the annual and seasonal mean climate for Kiribati Line Group under four emissions scenarios; RCP2.6 (very low emissions, in dark blue), RCP4.5 (low emissions, in light blue), RCP6 (medium emissions, in orange) and RCP8.5 (very high emissions, in red). Projected changes are given for four 20-year periods centred on 2030, 2050, 2070 and 2090, relative to a 20-year period centred on 1995. Values represent the multi-model mean change, with the 5–95% range of uncertainty in brackets. Confidence in the magnitude of change is expressed as *high*, *medium* or *low*. Surface air temperatures in the Pacific are closely related to sea-surface temperatures (SST), so the projected changes to air temperature given in this table can be used as a guide to the expected changes to SST. (See also Section 1.5.2). 'NA' indicates where data are not available.

Variable	Season	2030	2050	2070	2090	Confidence (magnitude of change)
Surface air temperature (°C)	Annual	0.7 (0.5–0.9)	0.8 (0.6–1.3)	0.8 (0.5–1.3)	0.8 (0.5–1.3)	*Medium*
		0.7 (0.5–1.1)	1.1 (0.7–1.6)	1.3 (0.9–1.9)	1.5 (1–2.3)	
		0.6 (0.4–0.9)	1 (0.6–1.4)	1.3 (0.9–1.9)	1.7 (1.1–2.5)	
		0.8 (0.6–1.1)	1.4 (1–2)	2.2 (1.5–3.2)	2.9 (2–4)	
Maximum temperature (°C)	1-in-20 year event	0.7 (0.2–1)	0.8 (0.3–1.4)	0.8 (0.1–1.6)	0.8 (0.3–1.3)	*Medium*
		0.6 (-0.1–1)	0.9 (0.3–1.5)	1.1 (0.1–1.8)	1.4 (0.8–2.2)	
		NA (NA–NA)	NA (NA–NA)	NA (NA–NA)	NA (NA–NA)	
		0.9 (0.3–1.4)	1.5 (0.8–2.3)	2.3 (1–3.7)	3 (1.7–4.4)	
Minimum temperature (°C)	1-in-20 year event	0.6 (0.2–0.7)	0.8 (0.4–1.1)	0.8 (0.3–1.3)	0.8 (0.4–1.2)	*Medium*
		0.6 (0.1–0.9)	0.9 (0.6–1.3)	1.2 (0.4–1.6)	1.4 (0.7–2)	
		NA (NA–NA)	NA (NA–NA)	NA (NA–NA)	NA (NA–NA)	
		0.8 (0.4–1.3)	1.4 (0.8–2)	2.3 (1.5–3.3)	3 (2–3.9)	
Total rainfall (%)	Annual	2 (-5–7)	5 (-4–14)	6 (-2–14)	6 (-3–14)	*Low*
		5 (-5–16)	6 (-2–15)	7 (-8–15)	11 (1–20)	
		4 (-5–10)	5 (-3–12)	5 (-4–15)	7 (-2–18)	
		5 (-1–11)	9 (-2–19)	13 (0–26)	16 (2–30)	
Total rainfall (%)	Nov-Apr	3 (-5–8)	7 (-5–15)	8 (2–17)	8 (-5–18)	*Low*
		6 (-8–15)	9 (-2–19)	9 (-13–21)	12 (2–22)	
		5 (-5–13)	7 (-2–16)	7 (-6–19)	8 (-3–23)	
		7 (-1–17)	11 (-1–26)	16 (2–31)	18 (5–35)	
Total rainfall (%)	May-Oct	0 (-8–6)	2 (-9–12)	4 (-8–14)	3 (-8–11)	*Low*
		3 (-7–13)	3 (-7–12)	4 (-5–14)	8 (-4–18)	
		1 (-10–8)	0 (-9–9)	2 (-11–13)	4 (-10–15)	
		2 (-6–9)	5 (-4–14)	9 (-7–20)	14 (-3–29)	
Aragonite saturation state (Ωar)	Annual	-0.3 (-0.5–-0.1)	-0.4 (-0.6–-0.2)	-0.4 (-0.6–-0.2)	-0.3 (-0.5–-0.1)	*Medium*
		-0.3 (-0.5–-0.1)	-0.5 (-0.7–-0.3)	-0.6 (-0.8–-0.4)	-0.7 (-0.9–-0.4)	
		NA (NA–NA)	NA (NA–NA)	NA (NA–NA)	NA (NA–NA)	
		-0.3 (-0.6–-0.1)	-0.6 (-0.8–-0.4)	-1.0 (-1.2–-0.8)	-1.3 (-1.5–-1.1)	
Mean sea level (cm)	Annual	12 (7–17)	21 (13–29)	31 (18–44)	40 (23–59)	*Medium*
		12 (7–16)	22 (13–30)	33 (20–47)	46 (27–66)	
		11 (7–16)	21 (13–29)	33 (19–46)	47 (28–67)	
		12 (7–17)	24 (16–33)	40 (26–56)	61 (38–87)	

Waves Projections Summary

Table 6.8: Projected average changes in wave height, period and direction in the Gilbert Islands, Kiribati for December–March and June–September for RCP4.5 (low emissions, in blue) and RCP8.5 (very high emissions, in red), for two 20-year periods (2026–2045 and 2081–2100), relative to a 1986–2005 historical period. The values in brackets represent the 5th to 95th percentile range of uncertainty.

Variable	Season	2035	2090	Confidence (range)
Wave height change (m)	December–March	-0.0 (-0.2–0.1) -0.1 (-0.2–0.1)	-0.1 (-0.2–0.1) -0.2 (-0.3–0.1)	*Low*
	June–September	0.0 (-0.1–0.1) 0.0 (-0.1–0.1)	0.0 (-0.1–0.1) 0.0 (-0.1–0.1)	*Low*
Wave period change (s)	December–March	-0.0 (-1.0–1.5) -0.1 (-1.3–1.1)	-0.1 (-1.2–1.6) -0.2 (-1.3–1.5)	*Low*
	June–September	+0.1 (-0.5–0.7) 0.0 (-0.6–0.6)	+0.0 (-0.7–0.7) -0.0 (-0.7–0.7)	*Low*
Wave direction change (°clockwise)	December–March	0 (-10–10) 0 (-10–10)	0 (-10–10) 0 (-10–10)	*Low*
	June–September	+0 (-10–10) 0 (-10–10)	+0 (-10–20) +0 (-10–20)	*Low*

Table 6.9: Projected average changes in wave height, period and direction in the Phoenix Islands, Kiribati for December–March and June–September for RCP4.5 (low emissions, in blue) and RCP8.5 (very high emissions, in red), for two 20-year periods (2026–2045 and 2081–2100), relative to a 1986–2005 historical period. The values in brackets represent the 5th to 95th percentile range of uncertainty.

Variable	Season	2035	2090	Confidence (range)
Wave height change (m)	December–March	-0.0 (-0.3–0.2) -0.0 (-0.3–0.2)	-0.1 (-0.3–0.2) -0.1 (-0.4–0.2)	*Low*
	June–September	0.0 (-0.1–0.2) 0.0 (-0.1–0.1)	0.0 (-0.1–0.2) +0.0 (-0.2–0.2)	*Low*
Wave period change (s)	December–March	0.0 (-1.5–1.8) -0.1 (-1.4–1.6)	-0.1 (-1.8–2.0) -0.1 (-1.9–1.9)	*Low*
	June–September	+0.1 (-0.8–0.9) +0.0 (-0.8–0.9)	0.0 (-1.0–1.0) -0.0 (-1.0–0.9)	*Low*
Wave direction change (°clockwise)	December–March	0 (-20–20) 0 (-20–20)	-0 (-20–20) -0 (-20–20)	*Low*
	June–September	+0 (-10–10) 0 (-10–10)	0 (-10–10) +0 (-10–10)	*Low*

Table 6.10: Projected average changes in wave height, period and direction in the Line Islands, Kiribati for December–March and June–September for RCP4.5 (low emissions, in blue) and RCP8.5 (very high emissions, in red), for two 20-year periods (2026–2045 and 2081–2100), relative to a 1986–2005 historical period. The values in brackets represent the 5th to 95th percentile range of uncertainty.

Variable	Season	2035	2090	Confidence (range)
Wave height change (m)	December–March	-0.0 (-0.3–0.3) -0.0 (-0.3–0.2)	-0.1 (-0.4–0.2) -0.1 (-0.4–0.2)	*Low*
	June–September	0.0 (-0.2–0.2) +0.0 (-0.1–0.2)	0.0 (-0.2–0.2) +0.0 (-0.2–0.3)	*Low*
Wave period change (s)	December–March	0.0 (-1.5–1.8) -0.1 (-1.4–1.7)	-0.1 (-1.7–1.9) -0.1 (-1.8–2.0)	*Low*
	June–September	+0.0 (-0.9–1.0) 0.0 (-0.9–0.9)	0.0 (-1.0–1.0) +0.0 (-1.2–1.0)	*Low*
Wave direction change (° clockwise)	December–March	0 (-30–30) 0 (-20–20)	0 (-30–20) 0 (-30–30)	*Low*
	June–September	0 (-10–10) 0 (-10–10)	0 (-10–10) +0 (-10–10)	*Low*

Wind-wave variables parameters are calculated for a 20-year period centred on 2035.